Combined first-principles and EXAFS study of structural instability in $BaZrO_3$

A. I. Lebedev* and I. A. Sluchinskaya
Physics Department, Moscow State University, Moscow, 119991, Russia
(Dated: April 24, 2013)

Phonon spectrum of cubic barium zirconate is calculated from first principles using the density functional theory. Unstable phonon mode with the R_{25} symmetry in the phonon spectrum indicates an instability of the cubic structure with respect to rotations of the oxygen octahedra. It is shown that the ground-state structure of the crystal is $I4/mcm$. In order to find the manifestations of the predicted instability, EXAFS measurements at the Ba $L_{\rm III}$-edge are used to study the local structure of $BaZrO_3$ at 300 K. An enhanced value of the Debye–Waller factor for the Ba–O atomic pair ($\sigma_1^2 \sim 0.015$ Å^2) revealed in the experiment is associated with the predicted structural instability. The average amplitude of the thermal octahedra rotation estimated from the measured σ_1^2 value is ∼4 degrees at 300 K. The closeness of the calculated energies of different distorted phases resulting from the condensation of the R_{25} mode suggests a possible structural glass formation in $BaZrO_3$ when lowering temperature, which explains the cause of the discrepancy between the calculations and experiment.

PACS numbers: 77.84.-s, 61.50.Ks, 64.70.K-, 61.05.cj

I. INTRODUCTION

Crystals with a general formula ABO_3 and the perovskite structure form a large family whose characteristic feature is a tendency to various (ferroelectric, ferroelastic, magnetic, superconducting) phase transitions. Barium zirconate $BaZrO_3$, one of the members of this family, is a crystal with a high melting point (∼2600°C), moderate dielectric constant (∼40), low dielectric losses, and low thermal expansion coefficient. It is widely used as a material for microwave ceramic capacitors and for inert crucibles used for growth of single crystals of high-temperature superconductors. In recent years, the interest to barium zirconate has revived again because it was found that $BaZrO_3$ doped with acceptor impurities, in particular yttrium, is a high-temperature ionic conductor with high proton conductivity, which can be used in solid-oxide fuel cells.[1–4] Its solid solutions with $BaTiO_3$ are relaxors with a very high electric-field tuning of the dielectric constant;[5–7] this property can be used in tunable filters, oscillators, phase shifters, etc. It should be noted that up to now, the properties of $BaZrO_3$ have been studied mainly at room and higher temperatures. Only a few experiments[8] (in addition to the first-principles calculations[8–13]) were undertaken to study the properties of $BaZrO_3$ (the ground-state structure, the behavior of the dielectric constant, etc.) at low temperatures at which most perovskite oxides exhibit interesting properties.

Recent X-ray and neutron diffraction studies[8] did not found any phase transitions in $BaZrO_3$ at $T < 300$ K, so that barium zirconate retains the cubic $Pm3m$ structure down to very low temperatures (2 K). These structural data, however, disagree with the results of the first-principles phonon spectra calculations for $BaZrO_3$ (Refs. 8–10,12,13), in which the appearance of the unstable R_{25} mode indicates an instability of the cubic structure with respect to the rotation of the oxygen octahedra. In Ref. 10, the equilibrium low-symmetry $P\bar{1}$ structure was found, which results from the doubling the unit cell in all directions and the rotation of the ZrO_6 octahedra according to Glazer tilt system $a^-b^-c^-$. Taking into account of these rotations was shown to improve the agreement between the calculated values of the low-temperature dielectric constant with experiment.[10] An indirect indication of the possible phase transformation in $BaZrO_3$ crystals can be its very low thermal expansion coefficient at $T < 300$ K.[8] In order to explain the disagreement between the theory and experiment, it was suggested that, for some reason, the long-range order in the octahedra rotations in these crystals cannot be established even at low temperatures. In particular, it was supposed that it may be caused by zero-point lattice vibrations.[8,9,11]

The aim of this work is to calculate the phonon spectrum and the ground-state structure for $BaZrO_3$ from first principles and to find experimental evidence for the structural instability in this material. We started from the assumption that, even if the long-range order in barium zirconate is absent for some reason, the structural instability, if it exists, should be manifested in the change of the *local structure*. To search for these changes, the extended X-ray absorption fine structure (EXAFS) studies are used. EXAFS is one of the modern powerful experimental techniques that enables to obtain detailed information on the local structure of crystals.[14] We expected to find the evidence for the structural instability in $BaZrO_3$ from anomalous behavior of the Debye–Waller factors which characterize the magnitude of the local displacements and the amplitude of thermal vibrations.

II. CALCULATION AND EXPERIMENTAL TECHNIQUES

In this work, the calculations were performed from first principles using the density functional theory. The pseu-

dopotentials for Ba, Zr, and O atoms used in the calculation were borrowed from Refs. 15,16. The cut-off energy of plane waves was 30 Ha (816 eV). The integration over the Brillouin zone was performed on the 8×8×8 Monkhorst–Pack mesh. The lattice parameters and the equilibrium atomic positions were determined from the condition of decreasing of the residual forces acting on the atoms below $5 \cdot 10^{-6}$ Ha/Bohr (0.25 meV/Å) while the accuracy of the total energy calculation was better than 10^{-10} Ha. To calculate of the phonon spectra, the formulas derived from the density functional perturbation theory and the interpolation technique[15] were used. The calculated lattice parameter for the cubic $BaZrO_3$ was $a_0 = 4.1659$ Å and agreed well with the experimental value obtained at 10 K (4.191 Å, Ref. 8). The slight difference of these values was due to a systematic underestimation of the lattice parameter typical for the local density approximation (LDA) used in this work.

The sample of barium zirconate was prepared by the solid phase reaction method. The initial components were $BaCO_3$ and microcrystalline ZrO_2 obtained by the decomposition of $ZrOCl_2 \cdot 8H_2O$ at 300°C. The components were dried at 600°C, weighed in proper proportions, ground in acetone and calcined in air at 1100°C for 6 h. The resulting powder was ground again and annealed at 1500°C for 3 h. The single-phase character of the sample was confirmed by X-ray diffraction.

Four EXAFS spectra were recorded using the simultaneous registration of the transmission signal and X-ray fluorescence on the KMC-2 station of the BESSY synchrotron radiation source (the beam energy of 1.7 GeV, the beam current up to 300 mA) at the Ba $L_{\rm III}$-edge (5.247 keV) at 300 K. The intensity of the incident radiation was measured by an ionization chamber, the intensity of radiation transmitted through the sample was measured with a silicon photodiode, and the intensity of the X-ray fluorescence excited in the sample was measured using the RÖNTEC silicon energy-dispersive detector.

The Ba $L_{\rm III}$-edge was chosen for measurements because the expected structural instability, which is accompanied by the rotation of the oxygen octahedra, should manifest most strongly in the change of the Ba–O interatomic distances, and not in the Zr–O interatomic distances. This is because the Zr–O distances change very little when the octahedra are rotated. In principle, the rotation of the octahedra could be also observed at the Zr K-edge as the changes in the multiple-scattering contributions to the EXAFS spectra as proposed in Ref. 17.

The EXAFS spectra processing was carried out in the traditional way.[18] The spectra were independently proceeded, and the results were then averaged. Since, according to our theoretical predictions, the temperature of the expected phase transition is below 300 K, the structure of $BaZrO_3$ at room temperature is cubic, and so the structural instability should be manifested as enhanced Debye–Waller factors.

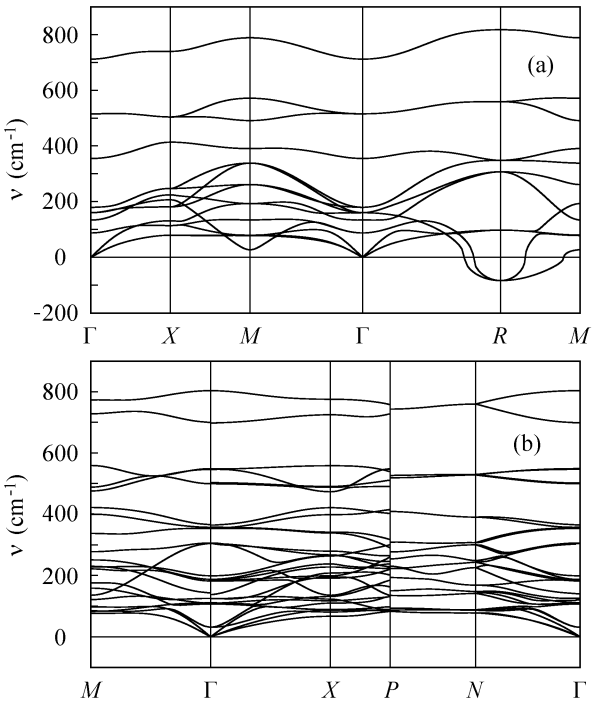

FIG. 1: Phonon spectrum of $BaZrO_3$ in the cubic $Pm3m$ phase (a) and the ground-state $I4/mcm$ phase (b).

TABLE I: The energies of different distorted phases of $BaZrO_3$. The energy of the cubic $Pm3m$ phase was taken as the energy reference.

Unstable mode	Glazer rotations	Space group	Energy (meV)
R_{25}	$a^-a^-a^-$	$R\bar{3}c$	−9.17
R_{25}	$a^0b^-b^-$	$Imma$	−9.47
R_{25}	$a^0a^0c^-$	$I4/mcm$	−10.01

III. RESULTS OF CALCULATIONS

The calculated phonon spectrum of $BaZrO_3$ with the cubic perovskite structure (space group $Pm3m$) is shown in Fig. 1a. It is seen that an unstable phonon with R_{25} symmetry (imaginary phonon energies are represented in the figure as negative values) appears in this spectrum. The eigenvector of the unstable phonon indicates that the cubic structure is unstable with respect to the octahedra rotations. The results of our calculations are consistent with the results of previous calculations,[8–10,12,13] but it should be noted that an additional instability at the M point, which was observed in Ref. 12, was not found in our phonon spectrum.

To determine the structure of the ground state, the energies of different distorted phases resulting from the condensation of triply degenerate unstable R_{25} mode were calculated. We write a Landau-type expansion of the to-

tal energy of a crystal in a power series of the amplitudes of the distortions,

$$E_{\rm tot} = E_{\rm tot}(0) + a(\phi_x^2 + \phi_y^2 + \phi_z^2) + b(\phi_x^2 + \phi_y^2 + \phi_z^2)^2 + c(\phi_x^4 + \phi_y^4 + \phi_z^4) + d(\phi_x^2 + \phi_y^2 + \phi_z^2)^3 + e\phi_x^2\phi_y^2\phi_z^2 + \dots , \quad (1)$$

where $E_{\rm tot}(0)$ is the total energy of the parent cubic phase, and ϕ_x, ϕ_y, and ϕ_z are the angles of rotation around three fourfold axes of the cubic structure. From this expansion it can be shown that to find the ground-state structure, it is sufficient to calculate the energies of phases described by the order parameters (ϕ,0,0), (ϕ,ϕ,0), and (ϕ,ϕ,ϕ), which correspond to the minimums of $E_{\rm tot}$ for different combinations of signs of the coefficients c and e. The specified order parameters correspond to the Glazer tilt systems $a^0a^0c^-$, $a^0b^-b^-$, and $a^-a^-a^-$, and lead to the $I4/mcm$, $Imma$, and $R\bar{3}c$ space groups, respectively. As follows from Table I, the $I4/mcm$ phase has the lowest energy among these phases. This phase can be obtained from the cubic $Pm3m$ structure by the out-of-phase rotation of the oxygen octahedra around one of the fourfold axes. The energy of this phase is ∼10 meV lower than the energy of the cubic phase; this gives an estimated phase transition temperature of ∼120 K. The calculations of the phonon spectrum (Fig. 1b) and elastic properties for the $I4/mcm$ phase prove that this phase is the ground-state structure.

It should be noted that among the obtained phases there is no $P\bar{1}$ solution, which was considered as the ground-state structure in Ref. 10. This phase corresponds to the Glazer tilt system $a^-b^-c^-$, in which the rotation angles around three fourfold axes of the cubic structure are different. The testing of this solution showed that the $P\bar{1}$ structure very slowly relaxes to the $I4/mcm$ solution found above (the convergence to this result required over 400 iterations). This demonstrates that the use of the information on the symmetry of the total energy can significantly (by more than 10 times) reduce the computation time needed to find the ground-state structure and guarantees a correct result.

The lattice parameters and atomic coordinates in the ground-state structure of $BaZrO_3$ are given in Table II.

IV. EXPERIMENTAL RESULTS

A typical EXAFS spectrum for the $BaZrO_3$ sample obtained at the Ba $L_{\rm III}$-edge at 300 K is shown in Fig. 2. The data analysis shows that the spectra are consistent with a model in which the structure of the sample is cubic. The structural parameters (interatomic distances and the Debye–Waller factors) for the first three shells are given in Table III. It is seen that the structural parameters obtained using two different measurement methods (transmission and fluorescence) are practically the same.

In Table III, it should be noted that the Debye–Waller factor for the first shell is much higher than the values for the second and third shells (usually the values of this factor increase monotonically with increasing interatomic distance).

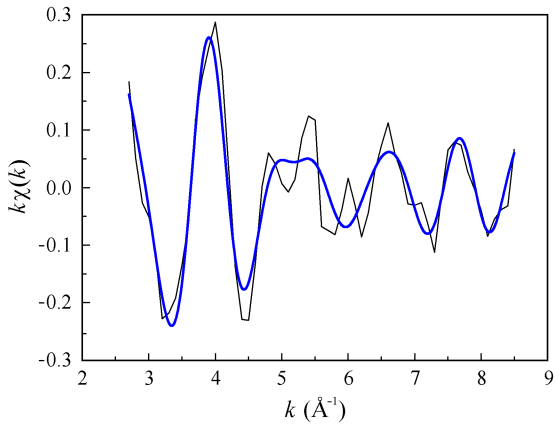

FIG. 2: (Color online) A typical EXAFS spectrum of $BaZrO_3$ obtained at the Ba $L_{\rm III}$-edge at 300 K (thin, black line) and the results of its fitting (thick, blue line).

The values of the Debye–Waller factors are determined by two components: (1) static distortions of the structure and (2) thermal vibrations. As our measurements are performed at a temperature above the temperature of the expected phase transition, the static distortions of the structure are absent. Furthermore, the optical modes responsible for the deformation of the oxygen octahedron are high-energy modes in the phonon spectrum of $BaZrO_3$ and are not excited at 300 K. Therefore, we can consider the octahedron ZrO_6 as a rigid unit. The thermal motion of the center of the octahedron relative to the Ba atom is characterized by the Debye–Waller factor σ_2^2. Since (as result of the rigidity of the octahedron) the oxygen atoms are strongly bound to the Zr atoms, the only way to explain why $\sigma_1^2 \gg \sigma_2^2$ is to take into account the rotation of the octahedra. Assuming that in the absence of the octahedra rotation the Debye–Waller factors for the Ba–O and Ba–Zr bonds are close (0.008 Å^2), the excess part of the Debye–Waller factor in the first shell, $\Delta\sigma_1^2 = \sigma_1^2 - \sigma_2^2$, can be associated with the thermal rotations. Then, using the formula

$$\Delta\sigma_1^2 = \frac{a_0^2\theta^2}{12},$$

which describes the dependence of $\Delta\sigma^2$ on the octahedra rotation angle θ about the fourfold axis of the cubic structure, we can estimate the amplitude of the thermal rotations. For the lattice parameter of $a_0 \approx 4.2$ Å, the mean rotation angle is $\sqrt{\theta^2} \approx 4°$. Taking into account the results of Ref. 19 in which the experimental value of the rotation angle in $SrTiO_3$ at 50 K (well below the temperature of the structural phase transition) is 2.01°, we can conclude the existence of the structural instability in $BaZrO_3$.

TABLE II: Calculated lattice parameters and atomic coordinates in the ground-state structure of $BaZrO_3$.

Phase	Lattice parameters (Å)	Atom	Wyckoff position	x	y	z
$I4/mcm$	$a = 5.8722$	Ba	$4b$	0.00000	0.50000	0.25000
	$c = 8.3577$	Zr	$4c$	0.00000	0.00000	0.00000
		O	$4a$	0.00000	0.00000	0.25000
		O	$8h$	0.22315	0.72315	0.00000

TABLE III: Structural parameters for the first three shells in cubic $BaZrO_3$ at 300 K obtained from the EXAFS data.

Measurement method	R_1 (Å)	σ_1^2 (Å^2)	R_2 (Å)	σ_2^2 (Å^2)	R_3 (Å)	σ_3^2 (Å^2)
Fluorescence	2.916	0.0155	3.640	0.0079	4.244	0.0101
Transmission	2.914	0.0145	3.635	0.0068	4.244	0.0087

V. DISCUSSION

Now, we discuss why the long-range order in the octahedra rotations is absent in $BaZrO_3$ at low temperatures. As was mentioned in Sec. I, one of the reasons for this behavior was the suppression of the long-range order by zero-point vibrations. In Ref. 20, a criterion was proposed, which enables, using a set of parameters obtained entirely from first principles, to estimate the stability of a structure with respect to zero-point vibrations. According to this criterion, zero-point vibrations prevent the system to be localized in one of the local minima of the potential if $h\nu/E_0 > 2.419$, where ν is the unstable phonon frequency and E_0 is the depth of the local minimum of the potential. In our calculations, for the unstable R_{25} mode $h\nu = 81.2i$ cm$^{-1} \approx 10$ meV and $E_0 \approx 10$ meV (Table I); therefore, zero-point vibrations should not suppress the structural distortions in barium zirconate. The phonon frequency of $79i$ cm^{-1} and the local minimum depth of 8 meV obtained for $BaZrO_3$ in Ref. 10 give the ratio $h\nu/E_0 \approx 1.2$, which is close to our value. The parameters $h\nu \approx 27i$ cm^{-1} and $E_0 = 1.5$ meV obtained in Ref. 8 are much lower and give $h\nu/E_0 \approx 2.2$, which is anyway lower then the critical value. Therefore, the explanation proposed in Ref. 8,9,11 that the suppression of the long-range order in $BaZrO_3$ is caused by zero-point vibrations seems unlikely. The fact that the influence of zero-point vibrations on the phase transition in $BaZrO_3$ is weaker than in $SrTiO_3$ is not surprising because the masses of both metal atoms in barium zirconate are larger.

The theoretical calculations performed in this work enable to propose another explanation for the absence of the long-range order in $BaZrO_3$ crystals in which the structural instability is expected. The closeness of the total energies of the $R\bar{3}c$, $Imma$, and $I4/mcm$ phases (Table I), which can result from the condensation of the R_{25} mode, but do not satisfy the group–subgroup relation, enables to suggest the appearance of the structural glass state when cooling the crystals. The internal strains and defects cause the appearance of different phases with close energies at different points of the sample, obviously resulting in the absence of the long-range order in the octahedra rotations. Moreover, the oxygen vacancies, which can be generated in $BaZrO_3$ quite easily, disturb the three-dimensional connectivity of the perovskite structure and can also contribute to the structural glass formation. The uniqueness of barium zirconate among other crystals with the perovskite structure results from the fact that the energy difference between the phases with different rotation patterns is only 0.84 meV (Table I), which is much less than in other investigated crystals (Table IV). In our opinion, this small energy difference may explain the tendency of $BaZrO_3$ to the formation of the structural glass.

TABLE IV: The minimum and maximum energies of the phases resulting from the condensation of rotational R_{25} and M_3 modes in some perovskite crystals and the difference of these energies.

Compound	Unstable mode	Space group	Energy (meV)	ΔE (meV)
$BaZrO_3$	R_{25}	$R\bar{3}c$	-9.17	0.84
	R_{25}	$I4/mcm$	-10.01	
$SrTiO_3$	M_3	$P4/mbm$	-9.5	21.4[15]
	R_{25}	$I4/mcm$	-30.9	
$CaTiO_3$	M_3	$P4/mbm$	-321	176[15]
	$R_{25} + M_3$	$Pbnm$	-497	
$CdTiO_3$	R_{25}	$I4/mcm$	-912	371[20]
	$R_{25} + M_3$	$Pbnm$	-1283	
$SrZrO_3$	R_{25}	$I4/mcm$	-298	69
	$R_{25} + M_3$	$Pbnm$	-367	

Further experiments on $BaZrO_3$, such as studies of the temperature dependence of the diffraction line width, diffuse scattering, elastic properties, and other physical

phenomena sensitive to the rotations of the octahedra, could provide additional information on the cause of the discrepancy between theory and experiment and to confirm or refute our explanation. We think that the low-temperature Raman studies of barium zirconate can also be very useful; our calculations show that five first-order Raman lines located at 16–36, 104–111, 121–128, 350–361, and 547–548 cm^{-1} appear in three possible distorted phases ($R\bar{3}c$, $Imma$, and $I4/mcm$) with the octahedra rotations.

VI. CONCLUSION

First-principles calculations of the phonon spectrum of $BaZrO_3$ performed in this work and experimental observation of the enhanced Debye–Waller factor for the Ba–O bonds in the EXAFS study of $BaZrO_3$ suggest that barium zirconate actually exhibits the structural instability associated with the rotations of the oxygen octahedra. It is shown that zero-point lattice vibrations are not the factor that prevents the establishing of the long-range order in the octahedra rotations. Very close energies of the phases with the different rotation patterns, which can result from the condensation of the R_{25} phonon, suggest a possible transition to the structural glass state when cooling $BaZrO_3$ samples. This explains the apparent contradiction between the theoretical predictions and the absence of the long-range order in the octahedra rotations observed in the experiment.

Acknowledgments

The calculations presented in this work were performed on the laboratory computer cluster (16 cores). The authors are grateful to the BESSY staff and to the Russian-German laboratory for the financial support during their stay at BESSY. This work was partially supported by the Russian Foundation for Basic Research grant No. 13-02-00724.

* swan@scon155.phys.msu.ru

[1] K. Kreuer, Annu. Rev. Mater. Res. **33**, 333 (2003).
[2] P. Babilo and S. M. Haile, J. Am. Ceram. Soc. **88**, 2362 (2005).
[3] F. Iguchi, N. Sata, and H. Yugami, J. Mater. Chem. **20**, 6265 (2010).
[4] D. Pergolesi, E. Fabbri, A. D'Epifanio, E. Di Bartolomeo, A. Tebano, S. Sanna, S. Licoccia, G. Balestrino, and E. Traversa, Nature Mater. **9**, 846 (2010).
[5] X. G. Tang, K.-H. Chew, and H. L. W. Chan, Acta Mater. **52**, 5177 (2004).
[6] T. Maiti, R. Guo, and A. S. Bhalla, Appl. Phys. Lett. **90**, 182901 (2007).
[7] Q. Zhang, J. Zhai, and L. B. Kong, J. Adv. Dielectrics **2**, 1230002 (2012).
[8] A. R. Akbarzadeh, I. Kornev, C. Malibert, L. Bellaiche, and J. M. Kiat, Phys. Rev. B **72**, 205104 (2005).
[9] W. Zhong and D. Vanderbilt, Phys. Rev. Lett. **74**, 2587 (1995).
[10] J. W. Bennett, I. Grinberg, and A. M. Rappe, Phys. Rev. B **73**, 180102(R) (2006).
[11] R. Kagimura, M. Suewattana, and D. J. Singh, Phys. Rev. B **78**, 012103 (2008).
[12] A. Bilić and J. D. Gale, Phys. Rev. B **79**, 174107 (2009).
[13] C. Zhu, K. Xia, G. R. Qian, C. L. Lu, W. Z. Luo, K. F. Wang, and J.-M. Liu, J. Appl. Phys. **105**, 044110 (2009).
[14] P. A. Lee, P. H. Citrin, P. Eisenberger, and B. M. Kincaid, Rev. Mod. Phys. **53**, 769 (1981).
[15] A. I. Lebedev, Phys. Solid State **51**, 362 (2009).
[16] A. I. Lebedev, Phys. Solid State **52**, 1448 (2010).
[17] B. Rechav, Y. Yacoby, E. A. Stern, J. J. Rehr, and M. Newville, Phys. Rev. Lett. **72**, 1352 (1994).
[18] A. I. Lebedev, I. A. Sluchinskaya, V. N. Demin, and I. H. Munro, Phys. Rev. B **55**, 14770 (1997).
[19] W. Jauch and A. Palmer, Phys. Rev. B **60**, 2961 (1999).
[20] A. I. Lebedev, Phys. Solid State **51**, 802 (2009).